Improved methods for calculating magnetic fields of charged-particle beams

Stanley Humphries, Ph.D.

Field Precision LLC
E mail: techinfo@fieldp.com
Internet: https://www.fieldp.com

1 Introduction

This report describes methods in the **Trak** program to find self-consistent, beam-generated magnetic fields. The modifications are helpful for general work with relativistic electron beams. They are critical for simulations of high-power microwave devices like the relativistic magnetron and the magnetically-insulated line oscillator. There are several reasons why such devices present a challenge for ray-tracing codes:

> The magnitudes of the beam-generated electric and magnetic fields are comparable to the applied fields.
>
> Electron motion is highly disordered.
>
> The reverse flow of ions could significantly affect the distributions of space-charge and current.
>
> Electron and ion flows determine the axial variation of current through the inner conductor.

Two-dimensional ray-tracing codes like **Trak** have long had the ability to determine complex electric-field distributions. The critical issue is how to determine the beam-generated azimuthal magnetic flux density B_θ for complex systems. The next section discusses the limitations of previous approaches. It introduces the method employed in **Trak**, assignment of model-particle currents to the facets of the electric-field conformal mesh. The method can address disordered particle motion and counterflow of electrons and ions. Sections 3–5 give details on 1) determining particle intersections with facets, 2) assigning current to facets in the beam propagation volume and along the inner boundary and 3) finding the distribution of included current and B_θ from the facet currents. Section 6 describes test calculations to confirm the method and to demonstrate its features.[1]

[1]Previous versions of **Trak** used the facet-assignment method described in S. Humphries, Laser and Particle Beams **18**, 601 (2000) for the calculation of beam-generated fields. Although this method is useful for ordered relativistic beams, it fails when there is strong radial current flow. Furthermore, the method to determine feed current on inner electrode boundaries is not flexible enough to handle magnetically-insulated flow.

2 Calculation strategies for beam-generated magnetic fields

In high-current relativistic electron flows, magnetic forces generated by the particles are comparable to electric forces. The calculation of the electric force is fundamentally the same in all two-dimensional ray-tracing codes. The procedure is to increment the space charge in elements traversed by the model particles. The increment is proportional to the current and residence time of the particle. The codes solve the Poisson equation with the added space charge and proceed to the next iteration of orbit tracking. In contrast, there is little commonality in the calculation of beam-generated magnetic fields. Several approaches have been pursued, each with its limitations. It is useful to review these limitation to understand the approach in **Trak**.

At first glance, finding the beam-generated magnetic flux density in a cylindrical system seems trivial. The value at the position of a model particle is given by

$$B_\theta(r,z) = \frac{\mu_0\ I_z(r,z)}{2\pi r}, \tag{1}$$

where I_z is the current enclosed inside r at position z. All the complexities of the calculation arise in finding the enclosed current. Early ray-tracing codes used trajectory counting, summing the current of model particles inside the current one. Although this method is valid for particle-in-cell codes, it has severe limitations in ray-tracing codes. Here, model-particle trajectories are calculated in sequence. Except for the special case of laminar beams, it is uncertain whether other particles will be inside or outside the current trace at different axial positions. Counting methods fail for the disordered particle motion in magnetically-insulated lines.

An improvement is to introduce a mesh to record the current distribution of the full set of rays during an iteration. This information is used to find magnetic forces in the next cycle. A simple regular mesh (box elements) that covers the beam propagation volume is suitable for a calculation such as the converging-beam electron gun of Fig. 1*a*. For a concave emitter, the enclosed current at all positions in the beam propagation volume arises solely from beam contributions. The regular-mesh approach fails for the geometry of Fig. 1*b* where the system includes a convex emitter and/or a target. For this solution class (which includes the magnetically-insulated line), a portion of the enclosed current is carried on the surface of electrodes inside the pulsed beam. Because the electrode currents supply the beam, their spatial distributions depend on the model-particle dynamics. To address this problem, **Trak** assigns particle currents to facets of the electric field mesh. This conformal mesh contains information on the shapes of interior electrodes.

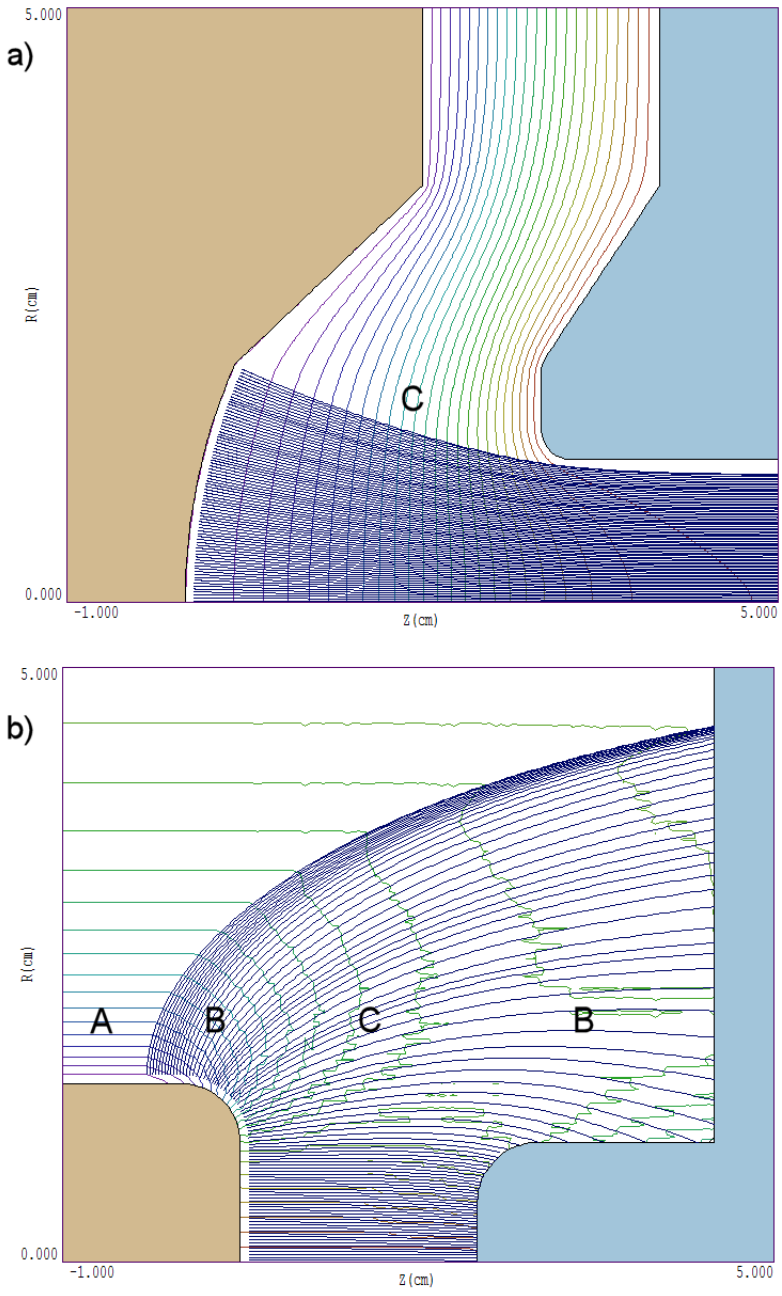

Figure 1: Calculation of beam generated fields. *a*) Converging beam gun with extraction aperture (model particle orbits and electrostatic contours). *b*) Convex cathode with target (model particle orbits and contours of B_θ). *A*) B_θ determined by current flow in electrodes. *B*) B_θ determined by beam current and current flow in electrodes. *C*) B_θ determined by beam current.

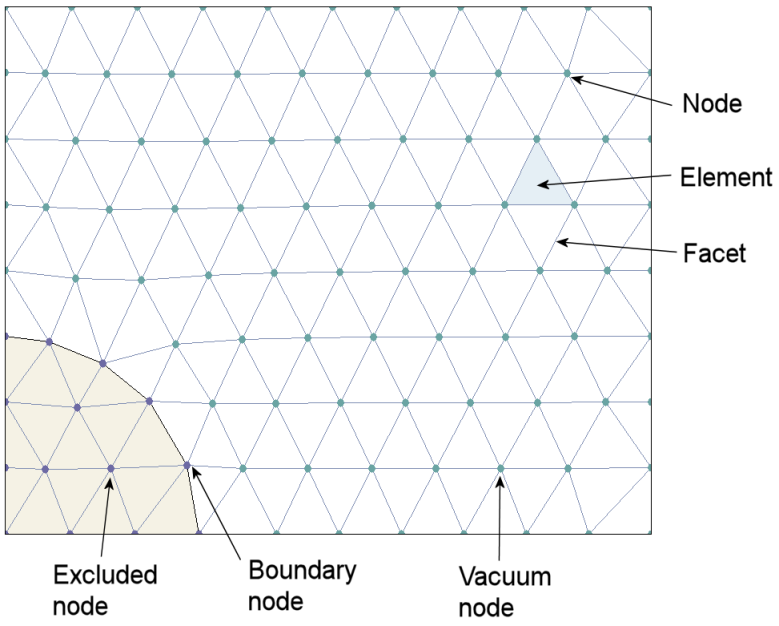

Figure 2: Definitions, structured conformal mesh of **Trak**. Clear elements represent vacuum. Colored elements represent an electrode.

Figure 2 illustrates the approach used is **Trak**. The solution space is divided into *elements* that define the division into electrodes and vacuum. *Nodes* are the vertices of the triangular mesh. We seek to determine I_z (an hence B_θ) at nodes. *Facets* are the boundaries between elements. Model-particle current is recorded on facets. An iteration cycle consists of the following stages:

Set facet currents to zero.

Track the set of particle orbits, assigning the model-particle current to intersected facets.

Interpret the facet currents to determine the enclosed current at nodes.

Calculate B_θ from Eq. 1 with averaging to ensure convergence.

There are two issues that complicate the analysis:

How to determine the sense of the facet current (positive or negative z) on a conformal triangular mesh.

How to set the current of facets on electrode surfaces to account for space-charge limited emission, target absorption, particle recapture and electron/ion counterflow.

Nodes, facets and elements have the *Vacuum* attribute over most of the **Trak** solution volume, Model particles move unimpeded through *Vacuum* elements. A *Vacuum* facet separates two *Vacuum* elements. A *Vacuum* node is surrounded by *Vacuum* elements. The inner boundary constitutes the second class of mesh components. The boundary may include the surface of an emission electrode, a portion of the axis and the surface of a target electrode. Alternatively, the inner boundary could be the shaped surface of a single electrode, as in the magnetically-insulated line. *Boundary* facets may lie along the axis ($r = 0.0$) or may separate a *Vacuum* element from the fixed-potential element of an electrode. *Boundary* nodes are connected by *Boundary* facets. Nodes that are surrounded by fixed-potential elements are in the class *Excluded*. These nodes do not participate in the calculation of included current. Finally, electrodes that are outside the radial extent of the particle flow are ignored because they do not affect the internal azimuthal field and the particle trajectories.

The next section describes a method to determine facet intersections for the vectors that constitute the trajectory of a model particle. Methods to find included current for *Boundary* nodes and facets are different from those used for *Vacuum* nodes and facets. Section 4 covers rules to set currents for *Boundary* facets. Section 5 reviews current assignment to *Vacuum* facets and methods to find included current and azimuthal field over the region of particle propagation.

3 Facet intersections

A trajectory calculation in **Trak** generates a series of vectors in space, with start point (X_s, Y_s, Z_s) and end point (X_e, Y_e, Z_e). This vector is converted to a line in the two-dimensional space of the electric field solution. For a cylindrical solution, the conversion is

$$z = Z, \tag{2}$$

$$r = \sqrt{X^2 + Y^2}. \tag{3}$$

Trak includes fast routines to identify the element occupied by a point (z, r). If the start and end points are in the same element, the orbit segment does not intersect a facet. If the points are in adjacent elements, the segment crosses the common facet. It is easy to check for adjacent elements using index operations on the structured meshes used for electric and magnetic fields in **Trak**.

Because of differences in time step and element size, it is possible that an orbit segment crosses several facets. The following recursive algorithm ensures that current is assigned to all intersected facets:

Define a last-in/first-out vector stack. Each stack entry contains the start and end points of a vector, (z_s, r_s, z_e, r_e).

Push the initial trajectory vector on the stack and enter a loop.

Check the start and end points of the last vector on the stack. If they are in the same element, pop the vector. If they are in adjacent elements, assign current to the common facet and pop the vector. In either case, exit the routine if there are no more stack entries. Otherwise, return to the start of the loop.

If the points of the last stack entry are not adjacent, then pop the vector and bifurcate it. Push the two vectors on the stack and return to the start of the loop.

The procedure works back from the end of the orbit vector, dividing it until the points of the last stack entry are either in the same or adjacent elements. The advantage of the stack approach is speed. It requires only index operations, with no geometric calculations to find vector-facet intersections.

4 Boundary facet currents

There are two options in **Trak** to create model particles:

Specification of the species, kinetic energy, initial position, initial direction and current for each model particle in the form of a list in the input file.

Automatic generation from Child-law emission surfaces.

In both cases there is an option to assign an axial orientation (*Pos* or *Neg*) to particles for relativistic beam calculations. In the default *Pos* mode, particles emerge from an upstream electrode or the left-hand boundary (z_{min}) and are collected on a downstream electrode or the right-hand boundary (z_{max}). The *Zero point* is a location on the inner boundary that separates the region of particle creation from the region of collection. Identification of the *Zero point* is easy for the calculations of Fig. 1 where the inner boundary contains source and collection electrodes separated a vacuum region. Here, the *Zero point* may be assigned to any location on the axis. When the inner boundary consists of a single electrode, if may be necessary to determine the *Zero point* with iterative calculations. In some cases the *Zero point* may represent only an approximation.

The new version of **Trak** uses the following procedure to locate and to mark the facets and nodes of inner boundaries of arbitrary shape. Starting

at the *Zero point*, the code walks in the -z direction. It collects the six nodes of the structured mesh connected to the present point. **Trak** steps to a node if 1) it is not the previous point and 2) the connecting facet separates a *Vacuum* element from either a fixed-potential element or an element outside the solution volume. On the first step, the additional condition that the new point must have a lower z coordinate is enforced. In this way, **Trak** walks backward along the axis and along the surface of any connected set of electrode elements until it reaches the boundary at z_{min} or r_{max}. A second search starts at the *Zero point* and moves in the positive z direction.

A particle crosses a *Boundary* facet if the start point is in a *Vacuum* element and the end point is in an electrode element (fixed potential). Particles cross *Boundary* facets when they terminate on a target. For emission surfaces, **Trak** uses the Child-law method described in S. Humphries, J. Computational Phys. **125**, 448 (1996). Trajectories are initiated on a virtual surface near the physical emission surface. Before starting a forward integration, the code backtracks the orbit to set space charge in the virtual gap. This feature is advantageous for the included current calculation because particles also penetrate the emission surface[2] The following rules govern assignment of current to boundary facets:

> Start with the current associated with the model particle (negative for electrons, positive for ions).
>
> Multiply the value by -1.0 if the axial orientation is *Neg*.
>
> Multiply by -1.0 if 1) the orbit is not in the *Backtrack* mode and 2) the facet lies on the source region for the particle. This operation accounts for the possibility that the model particle returns to its source (the currents assigned at creation and termination cancel).

Note that the sign of the current does not depend on the particle direction of motion.

When particle tracking in a cycle is complete, **Trak** calculates the included current along the inner boundary to represent current flow in electrodes. The code starts from the *Zero point* with $I_z = 0.0$ A and walks toward z_{min}. Facets on the axis carry no current so that the included current equals 0.0 at all positions. When **Trak** encounters an electrode, it walks outward, adding facet currents over emission regions. The included current equals the total beam current on the outer edge of the emission region and remains constant as the code completes the walk. A similar walk in the $+z$ direction ensures that a target carries the current of the intercepted fraction of the beam.

[2]There is an option to add a *BackTrack* option for list particles starting near a source electrode, in which case they effectively penetrate the boundary facets.

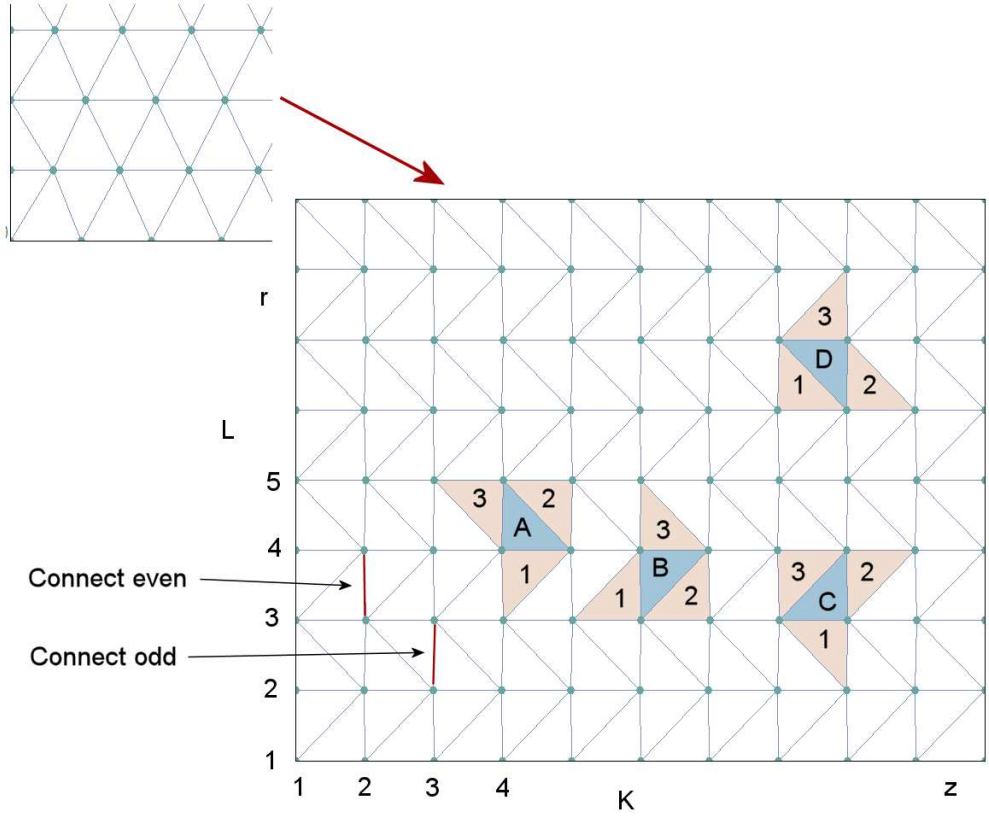

Figure 3: Visualization of the logic of a structured conformal triangular mesh to determine the direction of facet currents and connections for calculating the included current.

5 Vacuum facets and total included current

Current assigned to vacuum facets represents direct contributions from the beam. It is not immediately obvious how to interpret the direction of axial current and how to find the total included current at the nodes of a conformal triangular mesh (left side of Fig. 3). It would be difficult to define a consistent system on an unstructured triangular mesh, but the resolution is simple on the structured meshes used in **Trak**. The key to understanding the method is to shift nodes to display the logical mesh as a set of right-angle triangles as in Fig. 3. The logical mesh has a rectangular pattern with two elements inside each box. It is clear that the difference of included current between nodes in different rows equals the current of the vertical connecting facet (shown in red). The identity of the facets depends on whether the outer node is in an even or odd row. The direction of axial current flow depends on the relative positions of the start and end elements on the logical mesh.

Figure 3 shows the four possible arrangements of start (blue) and end (red) elements on the **Trak** mesh: *A*) the start element is the upper element with respect to a node on an even row, *B*) the start element is a lower element with respect to a node on an even row, *C*) the start element is an upper element with respect to a node on an odd row and *D*) the start element is a lower element with respect to node on an odd row. In each case, there are three possible adjacent end elements. For example, in Case *A* we ignore transitions to Element 1 and 2 and add the particle current multiplied by -1.0 to the common facet with Element 3. Here, the particle moves in the -z direction with respect to the logical mesh. For Case *C*, we ignore transitions to Elements 1 and 3 and add the current to the facet common with Element 2. The assigned currents are multiplied by an additional factor of -1.0 if the axial orientation of the particles is *Neg*.

The complete process for calculating the beam-generated magnetic field consists of the following steps:

> Track all particle orbits assigning current to boundary and vacuum facets according to the rules that have been described.
>
> Set values of included current along the nodes of the inner boundary by performing walks in the -z and +z directions from the *Zero point*.
>
> Loop over the mesh to set the included current of *Vacuum* nodes. moving outward in r (from $L = 2$ to L_{max}). The included current equals the value at the inner node connected by a vertical facet plus the facet current.
>
> Determine values of B_θ from the included current.

In the final step, an averaging factor ζ is used aid convergence by reducing oscillations between cycles:

$$B_\theta^{n+1} = (1-\zeta)B_\theta^n + \frac{\mu_0}{2\pi r}\,\zeta I_z^{n+1}. \tag{4}$$

The averaging factor is in the range $0.0 < \zeta < 1.0$. Low values give strong averaging.

6 Test calculations

This section reviews two calculations: a benchmark test (`BEAMMAGTEST`) and an application example for a magnetically-insulated line (`MIDEMO`). The benchmark calculation illustrates a simple yet sensitive test to confirm the validity of the complex procedure. Figure 4 shows the geometry. Electrons extracted from a concave emitter travel to a grounded vacuum chamber. There are no cathode-temperature effects, ensuring that electron flow is laminar (*i.e.*, orbits do not cross). In this case, contour lines of included current should exactly follow the trajectories of model particles.

The applied cathode voltage is -100 kV. An emission region covers the front and outer surfaces of the cathode. The zero point is at (0.10 m, 0.0 m). In Fig. 4, model electron trajectories are plotted in green. The backtracked portion of the trajectories is not plotted to show the location of the virtual emission surface. The space-charge-limited current converges to 621.41 after 20 cycles. Figure 4*a* shows the full set of model particle trajectories (green) and contours of B_θ (black). The irregularities in the contours result from interpolations on the discrete mesh (element size $\sim$ 0.2 mm). The peak value of flux density occurs on the connecting rod of radius 0.02 m. The peak value in the contour plot is close to the value predicted by Eq. 1 of 6.214 mtesla. The bottom figure shows contours of included current. For clarity, only half of the model particles are included. Within the resolution set by the mesh, the included-current contours closely follow the particle trajectories.

The complex electron flow in the second example demonstrates the versatility of the **Trak** method. A coaxial transmission line has inner radius $R_i = 0.075$ m and outer radius $R_o = 0.100$ m. A voltage -1.0 MV is applied to the center conductor. The solution volume covers the axial range -0.075 m $\leq z \leq$ 0.075 m. An electron emission region covers the inner conductor from $z = -0.070$ m to -0.020 m. The zero point location is (-0.02 m, 0.075 m). There is no applied axial magnetic field or ion flow. The magnetic flux density B_θ generated by the beam is supplemented with an applied flux density created by a bias current of -80.0 kA flowing in center conductor.

Figure 5a shows model electron orbits and contour lines of electrostatic potential. The total emitted electron current is 43.43 kA. The pattern of electron emission is quite complex. Electrons from the upstream end of the source are bent by the magnetic force, causing an accumulation of space-charge that suppresses emission from the downstream end. This plot does not give an accurate sense of current distribution because there are large variations in current weighting of model particles assigned at the emission surface. Figure 5*b*, showing the variation of B_θ, gives a better display of the current distribution. In particular, it shows that the particles that strike the

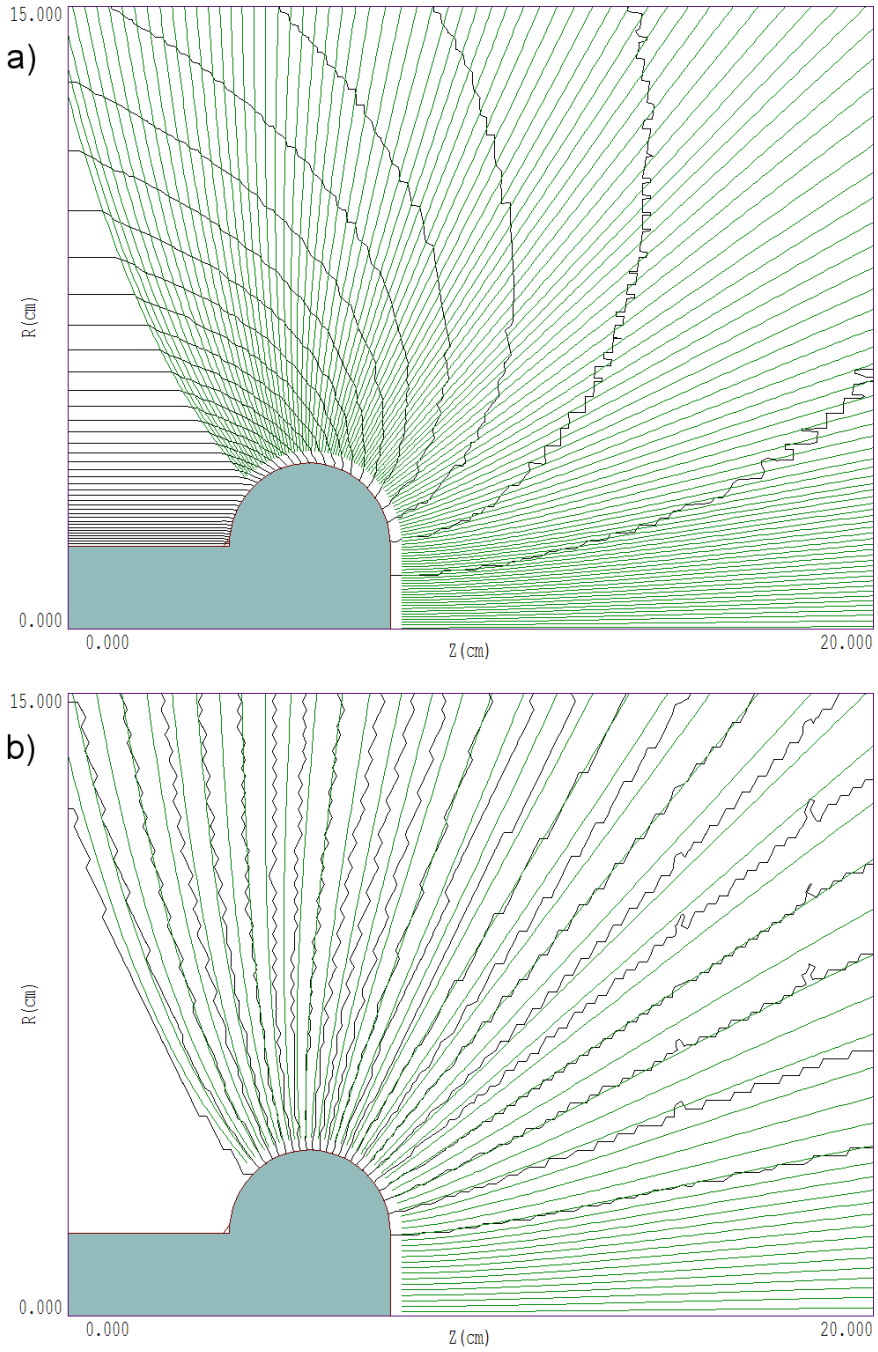

Figure 4: Example `BEAMMAGTEST`, electron extraction from a concave emitter. *a*) Model-particle orbits (green) and contours of B_θ (black). b) Selected model-particle orbits and contours of I_z,

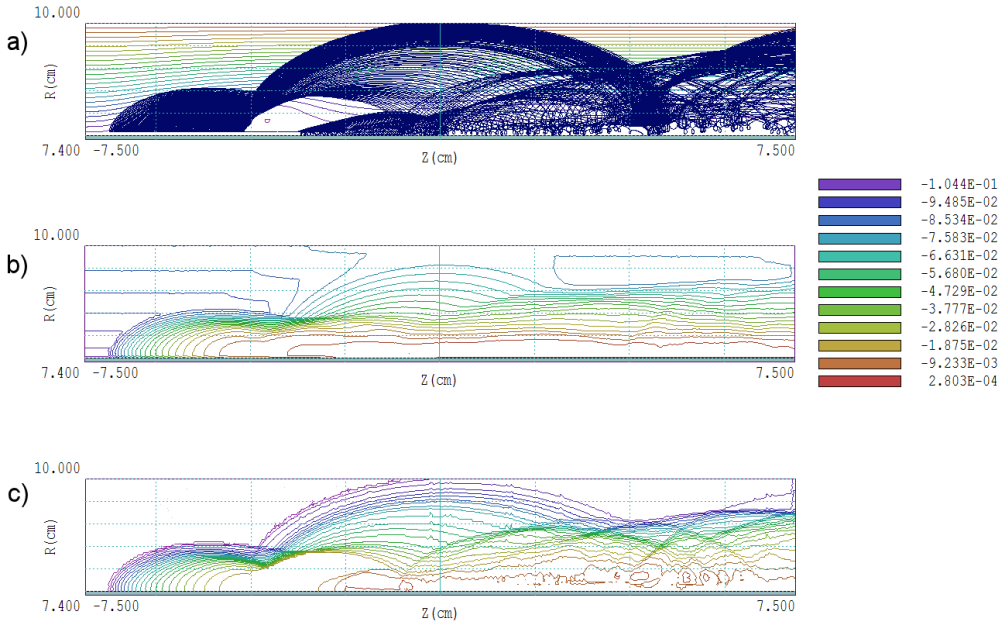

Figure 5: Example `MIDEMO`, magnetically-insulated line with a simple emission surface. *a*) Model-particle orbits and contours of electrostatic potential ϕ. *b*) Contours of B_θ. *c*) Contours of I_z.

outer conductor near $z = 0.0$ m carry only a small fraction of the current. Figure 5*c* provides an even better display. The included current I_z plot follows the nuances of the particle orbits and shows the actual distribution of axial current. The electron distribution settles into a parapotential-type flow near the exit boundary. Electrons at the boundary carry 38.78 kA (89% of the emitted current) and have an average kinetic energy 0.388 MeV.